materials

MDPI

Article

Novel Composite Electrolytes of $Zr_{0.92}Y_{0.08}O_{2-\alpha}$(8YSZ)-Low Melting Point Glass Powder for Intermediate Temperature Solid Oxide Fuel Cells

Hongtao Wang *, Ruifeng Du, Ruijuan Shi and Junlong Liu

School of Chemical and Material Engineering, Fuyang Normal College, Anhui Provincial Key Laboratory for Degradation and Monitoring of Pollution of the Environment, Fuyang 236037, China; ruifengdu1@163.com (R.D.); rjshi@fync.edu.cn (R.S.); jlliu@fync.edu.cn (J.L.)

* Correspondence: hongtaoking3@163.com; Tel.: +86-558-2596-249; Fax: +86-558-2596-703

Received: 19 June 2018; Accepted: 13 July 2018; Published: 16 July 2018

Abstract: In this study, $Zr_{0.92}Y_{0.08}O_{2-\alpha}$(8YSZ) powders were synthesized by the sol-gel method. The chemical physics changes and phase formation temperature of 8YSZ crystal were determined by thermogravimetry analysis and differential scanning calorimetry (TGA-DSC). 8YSZ-low melting point glass powder (8YSZ-glass) composite electrolytes with various weight ratios were prepared and calcined at different temperatures. The X-ray diffraction (XRD) patterns of the composite electrolytes were tested. The effects of synthesis temperature, weight ratio, test temperature, and oxygen partial pressure on the conductivities of 8YSZ-glass composite electrolytes, were also investigated at 400–800 °C. The result of the $\log\sigma$ ~$\log(pO_2)$ plot indicates that the 8YSZ-20% glass (700 °C) is almost a pure ionic conductor. The oxygen concentration discharge cell illustrates that the 8YSZ-20% glass (700 °C) composite electrolyte is a good oxygen ion conductor.

Keywords: defects; electrolyte; fuel cell; ceramics; sol-gel preparation

1. Introduction

ZrO_2-based electrolytes doped, with rare earth metallic cations, are excellent oxide ionic conductors, and they are widely used in oxygen sensors and solid oxide fuel cells (SOFCs) [1–4] due to their good mechanical strength and high ionic transport numbers. During the past decades, continuous research concentrating on Y_2O_3-stabilized ZrO_2 (YSZ) has been done [5,6]. For example, Caruso et al. investigated the influence of different parameters on the morphology and microstructure of YSZ powders synthesized by the sol-gel method [5].

However, SOFCs using YSZ as electrolyte membrane usually run at high temperatures (800–1000 °C). Therefore, researchers have focused on two ways to lower the operating temperature of YSZ. One strategy is to use YSZ films, and the other way is to construct composite electrolytes, which may have the combined advantages of each component [7–11]. A few research reports have shown that the thin film fuel cells using YSZ as membrane electrolytes generated maximum power output densities of 200–400 $mW{\cdot}cm^{-2}$ at 800 °C [12–14]. Singh et al. reported that the YSZ-SDC (samarium doped ceria) composite electrolyte with a weight ratio 8.5:1.5 has a higher electrical conductivity than single material YSZ at 400–700 °C [9]. It is well known that silicate, borate, mica, and other glass systems are commonly used as sealing materials in fuel cell systems [15–18]. It may be expected that using silicate low melting point glass powder, as a sintering aid, as well as composite electrolytes with improved gas tightness, durability, and better component matching, could be synthesized.

In this study, novel composite electrolytes of $Zr_{0.92}Y_{0.08}O_{2-\alpha}$(8YSZ)-low melting point glass powder were synthesized. The morphology, structure, and intermediate temperature electrochemical properties of the composite electrolytes were investigated by a variety of methods.

2. Experimental

We initially synthesized $Zr_{0.92}Y_{0.08}O_{2-\alpha}$(8YSZ) electrolyte via a sol-gel method using citric acid as a chelating agent as reported previously [19]. All the reagents used are analytical-grade. Firstly, Y_2O_3 was dissolved in nitric acid and $Zr(NO_3)_4 \cdot 5H_2O$ was dispersed into distilled water. The solution was then mixed with citric acid and NH_4OH and evaporated at 90 °C to get a gel. After gelation and ashing treatment, the obtained ash was calcined at 700 °C, 1200 °C and 1550 °C for 6 h, respectively, to get $Zr_{0.92}Y_{0.08}O_{2-\alpha}$(8YSZ) powder. The low melting point glass powder was used as a sintering aid to form composite. The composition of the low melting point glass powder is Na_2O-CaO-SiO_2-ZnO (Taizhou Xinhai Special Materials Factory, 300 mesh, m.p. is 550 °C). 8YSZ and low melting point glass powder were mixed with a weight ratio of four to one and heated at 700 °C, 1200 °C and 1550 °C for 2 h, correspondingly. The composites with weight ratio of 8YSZ: low melting point glass powder = 9:1 and 7:3 were also synthesized at 700 °C. These results are summarized in Table 1.

Table 1. The samples synthesized with different synthesis temperature and weight ratio.

Sample	Synthesis Temperature	Abbreviation
$Zr_{0.92}Y_{0.08}O_{2-\alpha}$-10 wt% low melting point glass	700 °C	8YSZ-10% glass 700 °C
$Zr_{0.92}Y_{0.08}O_{2-\alpha}$-20 wt% low melting point glass	700 °C	8YSZ-20% glass 700 °C
$Zr_{0.92}Y_{0.08}O_{2-\alpha}$-30 wt% low melting point glass	700 °C	8YSZ-30% glass 700 °C
$Zr_{0.92}Y_{0.08}O_{2-\alpha}$-20 wt% low melting point glass	1200 °C	8YSZ-20% glass 1200 °C
$Zr_{0.92}Y_{0.08}O_{2-\alpha}$-20 wt% low melting point glass	1550 °C	8YSZ-20% glass 1550 °C

The chemical physics changes and phase formation temperature of 8YSZ crystal were determined by thermogravimetry analysis and differential scanning calorimetry (TGA-DSC) (TGA-DSC, Universal V 3.7A, TA Instruments, New Castle, DE, USA). The X–ray diffraction (XRD) (XRD, X'pert Pro MPD, Amsterdam, Netherlands)patterns of the above electrolytes were tested with a Panalytical X'Pert Pro MPD diffractometer. The morphology of the 8YSZ-20% glass (700 °C) was observed using a scanning electron microscope (SEM, S-4700, Hitachi, Tokyo, Japan) [20,21].

The conductivities vs. different synthesis temperature, test temperature, oxygen partial pressure and weight ratio in nitrogen atmosphere were tested with an electrochemical analyzer (CHI660E, Shanghai, China) at 400–800 °C. All the samples were ground into thin slices of 1.0–1.2 mm. A 20% palladium-80% silver paste with silver wires was used to fabricate the electrodes (area: 0.5 cm^2). Oxygen concentration discharge fuel cell and H_2/O_2 fuel cell using the 8YSZ-20% glass (700 °C) as electrolyte were constructed [22,23].

3. Results and Discussion

The TGA and DSC curves of the $Zr_{0.92}Y_{0.08}O_{2-\alpha}$(8YSZ) gel heated at 15 °C·min^{-1} in nitrogen atmosphere up to 1000 °C are shown in Figure 1. It can be seen that the TGA curve shows a weight loss about 7% from 35 °C to 130 °C corresponding to two weak endothermic peaks in DSC curve, which is attributed to the residual water in the 8YSZ gel [24,25]. About seventy percent of weight loss of 8YSZ gel occurred up to c.a. 500 °C. The first calcined temperature was fixed at 700 °C because there is almost no weight loss at 520 °C and above [26,27].

The XRD patterns of 8YSZ and 8YSZ-glass obtained with different weight ratio and calcined at different synthesis temperature are shown in Figure 2. Figure 2a shows the XRD patterns of the 8YSZ-glass with different weight ratio calcined at 700 °C, i.e., 0%, 10%, 20% and 30%. All the samples possess coexisting tetragonal and monoclinic phases, where tetragonal is the major phase. The XRD angles at 30.14°, 34.72° and 35.04° belong to the (101), (002), and (110) crystal planes of t-$Zr_{0.9}Y_{0.1}O_{1.95}$

(JCPDS 82-1241), respectively. From Figure 2b, when the synthesis temperature reaches 1200 °C and 1550 °C, the XRD patterns of 8YSZ are merely tetragonal structures. However, there are still a few obvious diffraction peaks of monoclinic structure in 8YSZ-20% glass calcined at 1200 °C and 1550 °C, respectively. Mori et al. observed that the Ti^{4+}-doped 8YSZ electrolyte transform from a pure cubic structure to two-phase compound containing small amount of tetragonal phase with increasing Ti content [28]. And a monoclinic-to-tetragonal phase transformation was found in 9 mol% MgO doped ZrO_2 above 1300 °C [29]. Therefore, it is probably the high synthesis temperature and 20% weight ratio of low melting point glass leads to the appearance of monoclinic phase. Besides, a diffraction peak is observed at $2\theta \approx 26°$ may be indexed to the SiO_2 (JCPDS 13-0026) or $Na_2Si_3O_7$ (JCPDS 38-0019). This indicates that the Na_2O-SiO_2 in low melting point glass changes from amorphous to crystalline at high temperature.

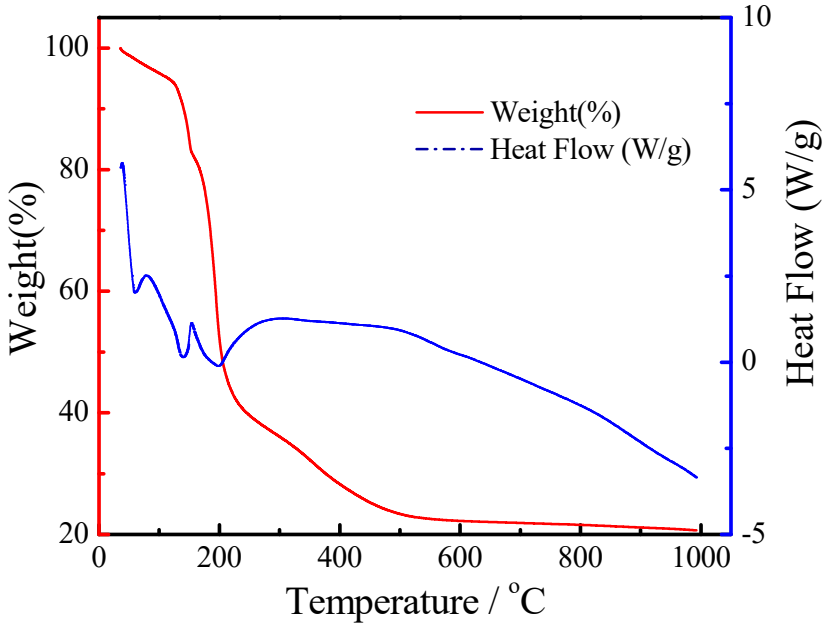

Figure 1. TGA-DSC test of the $Zr_{0.92}Y_{0.08}O_{2-\alpha}$(8YSZ) gel heated at 15 °C·min^{-1}.

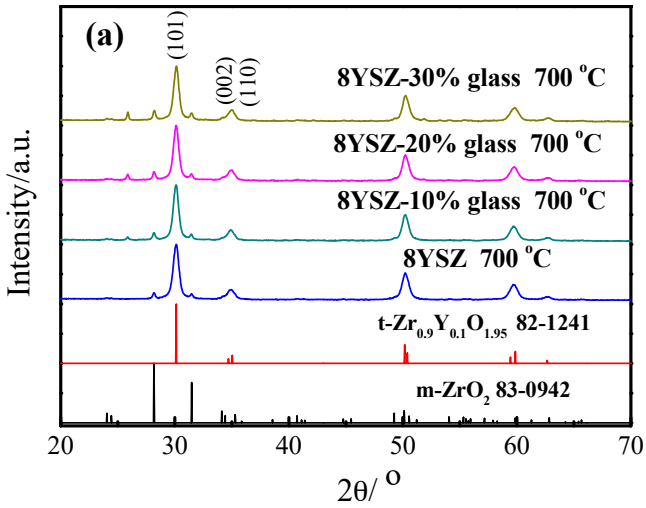

Figure 2. *Cont.*

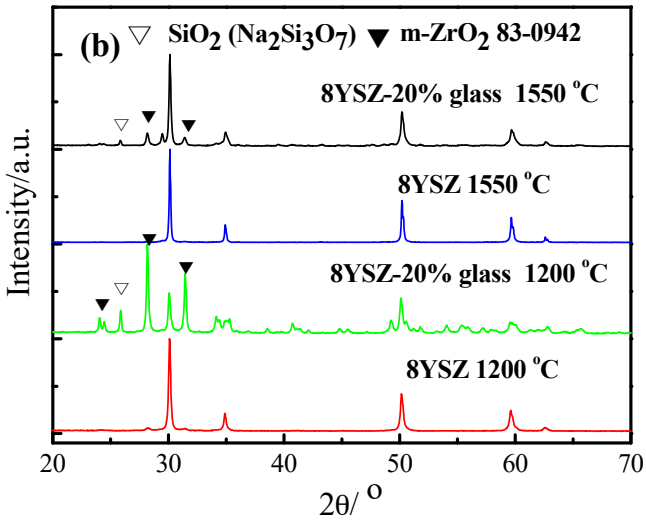

Figure 2. (**a**) XRD patterns of the 8YSZ, 8YSZ-10% glass, 8YSZ-20% glass and 8YSZ-30% glass calcined at 700 °C for 6 h; (**b**) XRD patterns of the 8YSZ and 8YSZ-20% glass calcined at 1200 °C and 1550 °C, respectively.

The conductivities vs. different synthesis temperature and weight ratio were tested at 400–800 °C in nitrogen atmosphere as shown in Figure 3. It is clear that the conductivities of composite electrolytes increase with the increase in glass concentration. And the highest conductivities are obtained for the 8YSZ-20% glass (700 °C), 8YSZ-20% glass (1200 °C), and 8YSZ-20% glass (1550 °C) to be 5.7×10^{-2} S·cm^{-1}, 4.1×10^{-3} S·cm^{-1}, and 2.3×10^{-2} S·cm^{-1} at 800 °C, respectively. A recent investigation by Lee et al. [29] reported that a single cubic phase of 8YSZ showed higher conductivity than 9 mol% MgO doped ZrO_2 which has a mixed phase. Similarly, the conductivities of the 8YSZ-20% glass (700 °C) (Figure 3a) and 8YSZ-20% glass (1550 °C) (Figure 3b) are higher than that of 8YSZ-20% glass (1200 °C) (Figure 3b) which has evidently tetragonal and monoclinic biphasic structure in Figure 2b. The conductivities of the 8YSZ-20% glass (700 °C) are lower than that of 8YSZ-30% glass (700 °C) composite electrolyte as shown in Figure 3a. However, the 8YSZ-30% glass (700 °C) composite electrolyte is unstable because it will cause segregation and reduce the mechanical hardness in the molten state when the glass powder is too high in percentage.

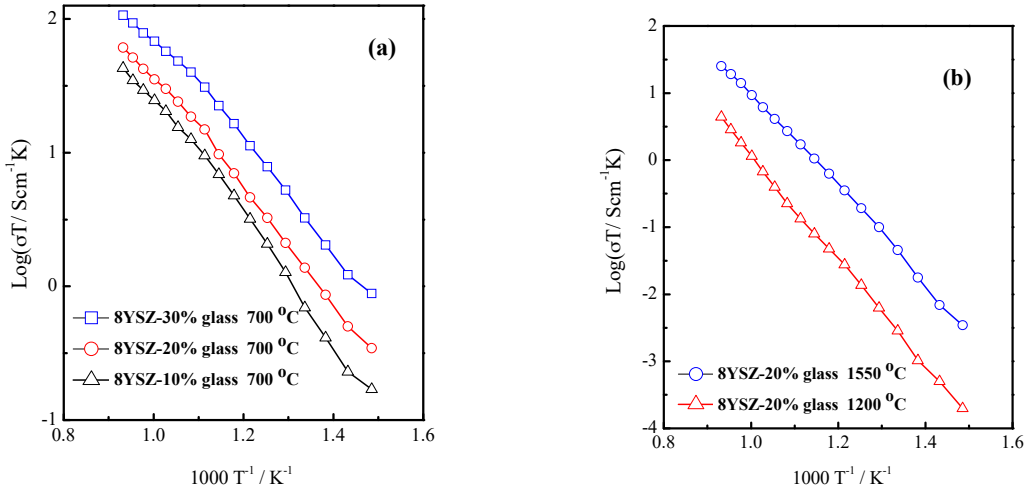

Figure 3. The conductivities vs. (**a**) different weight ratio of the 8YSZ-10% glass, 8YSZ-20% glass and 8YSZ-30% glass after calcined at 700 °C; (**b**) different synthesis temperature of the 8YSZ-20% glass (1200 °C, 1550 °C) in nitrogen atmosphere at 400–800 °C.

Figure 4 shows the variation of conductivity of 8YSZ-30% glass (700 °C) composite electrolyte with time in nitrogen atmosphere at 800 °C. The conductivity reaches a steady state in the first hour. However, with increasing time, the conductivity of 8YSZ-30% glass (700 °C) composite electrolyte gradually decreased. This suggests that it cannot be used for long period at 800 °C.

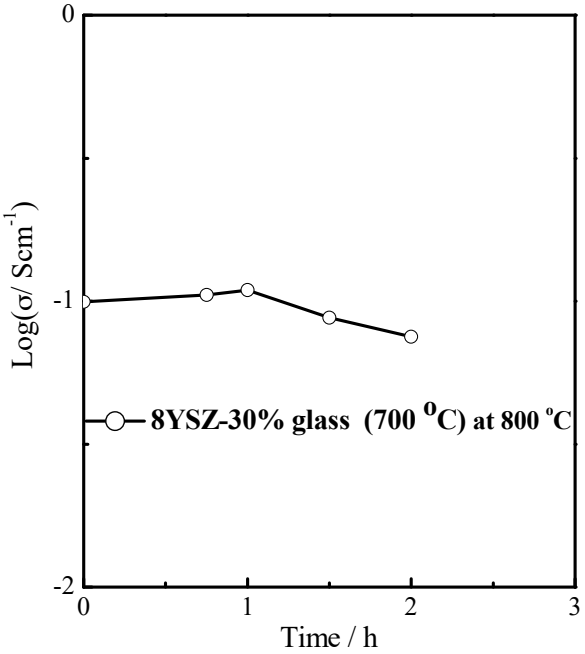

Figure 4. The variation of conductivity of 8YSZ-30% glass (700 °C) with time in nitrogen atmosphere at 800 °C.

The external (a) and cross-sectional (b) surface SEM images of the 8YSZ-20% glass (700 °C) composite electrolyte are displayed in Figure 5. The 8YSZ agglomerated with low melting point glass powder, few pores are observed and the microstructure is homogeneous after heating at 700 °C, which is attributed to high fluidity of molten glass. Figure 5 shows that the two components are evenly dispersed and intimately connected and do not react with each other due to their high chemical stability [3,5,9,11].

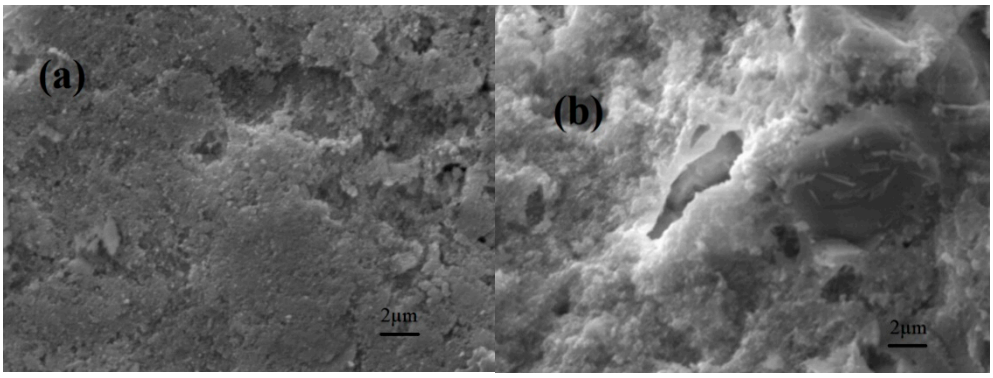

Figure 5. The external (**a**) and cross-sectional (**b**) surface SEM images of the 8YSZ-20% glass (700 °C) composite electrolyte.

In order to investigate ionic conduction of the 8YSZ-20% glass (700 °C), the relationship between the oxygen partial pressure (pO_2) and conductivities was studied. As shown in Figure 6, there is almost

a straight line within the whole pO_2 range. The result indicates that the 8YSZ-20% glass (700 °C) is almost a pure ionic conductor [20–23]. In the pO_2 range of 10^{-20}~10^{-15} atm, the curve is slightly upwarped, indicating that there is a trace electron conduction in the 8YSZ-20% glass (700 °C) in reducing atmosphere.

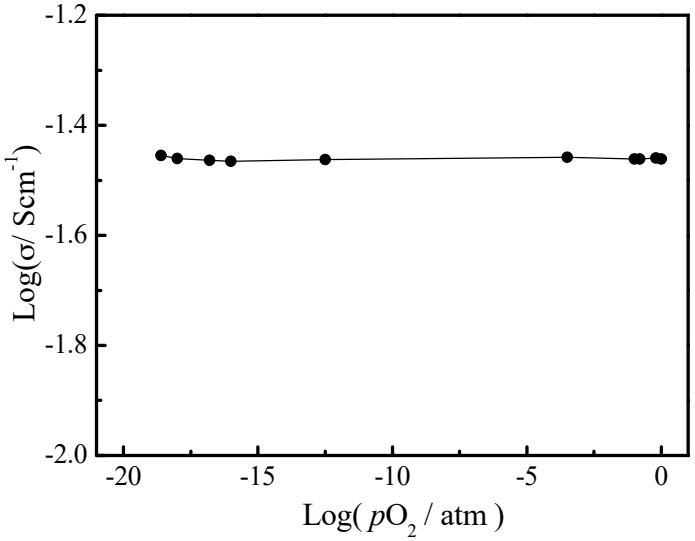

Figure 6. The conductivities of the 8YSZ-20% glass (700 °C) composite electrolyte as a function of pO_2 at 750 °C is almost a pure ionic conductor.

It is well known that ZrO_2-based electrolyte is a good oxygen ion conductor. To study the oxide ionic conduction of the 8YSZ-20% glass (700 °C) composite electrolyte, an oxygen concentration discharge cell was tested at 800 °C as shown in Figure 7. The calculational electromotive forces (EMF_{cal}) could be obtained from $EMF_{cal} = \frac{RT}{4F} t_O \ln[pO_{2\ (A)}/pO_{2\ (B)}]$ when $t_O = 1$. The air ($pO_{2\ (B)}$) and pure O_2 ($pO_{2\ (A)}$) are introduced into the anode and cathode, correspondingly. From Figure 7, the open circuit voltage is 35.6 mV, which is close to the calculated EMF (36.1 mV). Moreover, a stable discharge line could be seen in Figure 7. All the results illustrate that the 8YSZ-20% glass (700 °C) composite electrolyte is a good oxygen ion conductor.

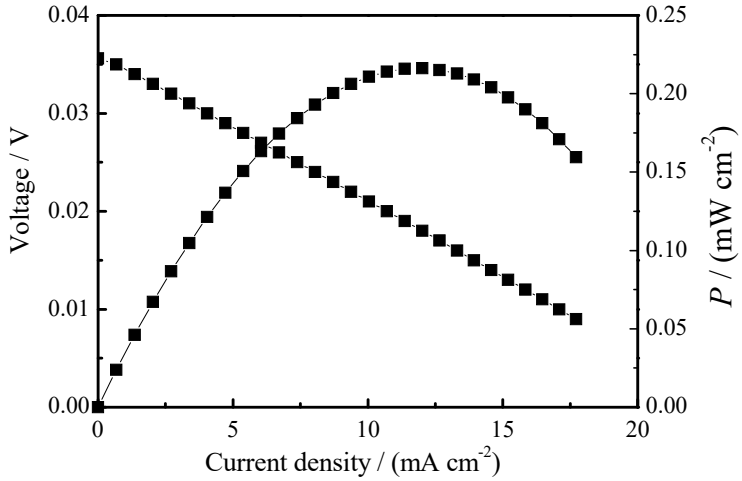

Figure 7. The oxygen concentration discharge cell: air, Pd-Ag | 8YSZ-20% glass (700 °C) | Pd-Ag, O_2 at 800 °C.

The H_2/O_2 fuel cell electrochemical performance was tested at 800 °C for the 8YSZ-20% glass (700 °C) as shown in Figure 8. It can be seen that the 8YSZ-20% glass (700 °C) reveals a high open circuit voltage (1.09 V) which means the composite electrolyte is dense [5]. The maximum power

density of the 8YSZ-20% glass (700 °C) is 72.7 mW·cm^{-2} (thickness = 1.1 mm) at 800 °C. The result is lower than that previous reported cathode supported thin film fuel cell with 200–400 mW·cm^{-2} at 800–850 °C [12–14,30], which can be attributed to the electrolyte thickness and the electrode/electrolyte interface. Further work is in progress to optimize the composition of composite electrolytes and develop the stable and high performance solid oxide fuel cell [31,32].

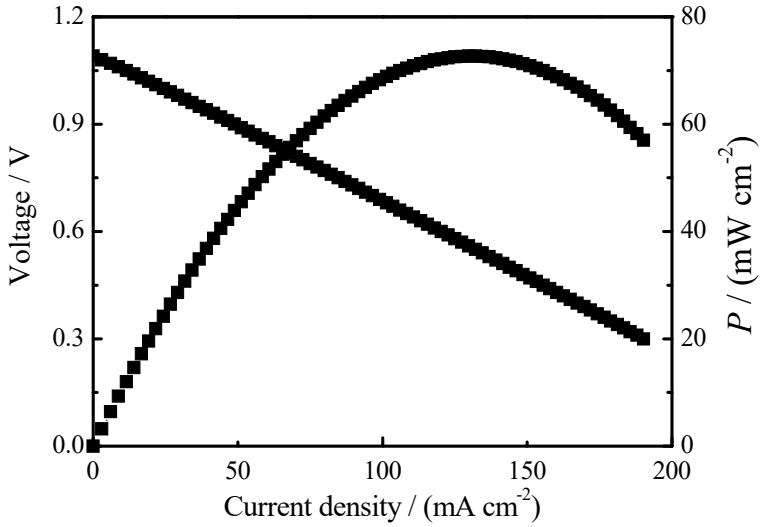

Figure 8. H_2/O_2 fuel cell of the 8YSZ-20% glass (700 °C) at 800 °C.

4. Conclusions

In this study, low melting point glass powder was chosen as a sintering aid to prepare novel $Zr_{0.92}Y_{0.08}O_{2-\alpha}$(8YSZ)-low melting point glass composite electrolytes. The results of XRD indicate that the major phase in composite electrolytes is tetragonal and no diffraction peaks of low melting point glass are found. The influences of amount of additive, synthesis temperature, test temperature, and oxygen partial pressure on the electrical conductivities of the composite electrolytes were investigated at 400–800 °C. The results of the XRD and conductivities show that the 8YSZ-20% glass (700 °C) is a suitable choice. The oxygen concentration discharge cell illustrates that the 8YSZ-20% glass (700 °C) composite electrolyte is a good oxygen ion conductor. The maximum power density of the 8YSZ-20% glass (700 °C) is 72.7 mW·cm^{-2} (thickness = 1.1 mm) at 800 °C.

Author Contributions: H.W. and R.D. conceived and designed the experiments; R.S. and J.L. performed the experiments; H.W. and R.D. analyzed the data; R.S. and J.L. contributed the used materials and analysis tools; H.W. and R.S. wrote the paper.

Funding: This work was supported by the National Natural Science Foundation (No. 51402052) of China. The Natural Science Project of Anhui Province (No. KJ2018A0337). Excellent Youth Foundation of Anhui Educational Committee (No. gxyq2018046). Research and innovation team horizontal cooperation project of Fuyang municipal government and Fuyang Normal College (No. XDHX2016019, XDHXTD201704. XDHX201739). Excellent Youth Foundation of Fuyang Normal College (rcxm201805).

Conflicts of Interest: The authors declare no conflicts of interest.

References

1. Chen, Y.; Orlovskaya, N.; Payzant, E.A.; Graule, T.; Kuebler, J. A search for temperature induced time-dependent structural transitions in 10 mol% Sc_2O_3-1 mol% CeO_2-ZrO_2 and 8 mol% Y_2O_3-ZrO_2 electrolyte ceramics. *J. Eur. Ceram. Soc.* **2015**, *35*, 951–958. [CrossRef]
2. Li, J.; Zhang, H.; Gao, M.; Li, Q.; Bian, W.; Tao, T.; Zhang, H. High-temperature wettability and interactions between Y-containing Ni-based alloys and various oxide ceramics. *Materials* **2018**, *11*, 749. [CrossRef] [PubMed]

3. Fondard, J.; Bertrand, P.; Billard, A.; Fourcade, S.; Batocchi, P.; Mauvy, F.; Bertrand, G.; Briois, P. Manufacturing and testing of a metal supported Ni-YSZ/YSZ/La_2NiO_4 ITSOFC synthesized by physical surface deposition processes. *Solid State Ion.* **2017**, *310*, 10–23. [CrossRef]
4. Xia, C.; Qiao, Z.; Feng, C.; Kim, J.; Wang, B.; Zhu, B. Study on zinc oxide-based electrolytes in low-temperature solid oxide fuel cells. *Materials* **2018**, *11*, 40. [CrossRef] [PubMed]
5. Mamana, N.; Díaz-Parralejo, A.; Ortiz, A.L.; Sánchez-Bajo, F.; Caruso, R. Influence of the synthesis process on the features of Y_2O_3-stabilized ZrO_2 powders obtained by the sol-gel method. *Ceram. Int.* **2014**, *40*, 6421–6426. [CrossRef]
6. Liu, Z.; Zhao, Z.; Shang, L.; Ou, D.; Cui, D.; Tu, B.; Cheng, M. LSM-YSZ nano-composite cathode with YSZ interlayer for solid oxide fuel cells. *J. Energy Chem.* **2017**, *26*, 510–514. [CrossRef]
7. Dankeaw, A.; Poungchan, G.; Panapoy, M.; Ksapabutr, B. In-situ one-step method for fabricating three-dimensional grass-like carbon-doped ZrO_2 films for room temperature alcohol and acetone sensors. *Sens. Actuators B Chem.* **2017**, *242*, 202–214. [CrossRef]
8. Liu, X.Y.; Xu, Z.H.; Liang, G.Y. Comparative study of the sintering behaviors between YSZ and LZ/YSZ composite. *Mater. Lett.* **2017**, *191*, 108–111. [CrossRef]
9. Raghvendra; Singh, P. Electrical conductivity of YSZ-SDC composite solid electrolyte synthesized via glycine-nitrate method. *Ceram. Int.* **2017**, *43*, 11692–11698. [CrossRef]
10. Bueta, F.R.; Imperial, J.F.; Cervera, R.B. Structure and conductivity of NiO/YSZ composite prepared via modified glycine-nitrate process at varying sintering temperatures. *Ceram. Int.* **2017**, *43*, 16174–16177. [CrossRef]
11. Elmouwahidi, A.; Bailón-García, E.; Pérez-Cadenas, A.F.; Maldonado-Hódar, F.J.; Castelo-Quibén, J.; Carrasco-Marín, F. Electrochemical performances of supercapacitors from carbon-ZrO_2 composites. *Electrochim. Acta* **2018**, *259*, 803–814. [CrossRef]
12. Moon, H.; Kim, S.D.; Hyun, S.H.; Kim, H.S. Characteristics of SOFC single cells with anode active layer via tape casting and cofiring. *Int. J. Hydrogen Energy* **2008**, *33*, 2826–2833. [CrossRef]
13. Song, J.H.; Park, S.I.; Lee, J.H. Fabrication characteristics of an anode-supported thin-film electrolyte fabricated by the tape casting method for IT-SOFC. *J. Mater. Process. Technol.* **2008**, *198*, 414–418. [CrossRef]
14. Rath, M.K.; Jung, Y.M.; Park, J.H.; Joh, D.W.; Lee, K.T. Heterogeneous nanograin structured NiO-YSZ anodes via a water-in-oil microemulsion route for solid oxide fuel cells. *J. Alloys Compd.* **2017**, *723*, 681–688. [CrossRef]
15. Habibnia, M.; Shakeri, M.; Nourouzi, S. Determination of the effective parameters on the fuel cell efficiency, based on sealing behavior of the system. *Int. J. Hydrogen Energy* **2016**, *41*, 18147–18156. [CrossRef]
16. Gödekea, D.; Dahlmann, U. Study on the crystallization behaviour and thermal stability of glass-ceramics used as solid oxide fuel cell-sealing materials. *J. Power Sources* **2011**, *196*, 9046–9050. [CrossRef]
17. Rautanen, M.; Pulkkinen, V.; Tallgren, J.; Himanen, O.; Kiviaho, J. Effects of the first heat up procedure on mechanical properties of solid oxide fuel cell sealing materials. *J. Power Sources* **2015**, *284*, 511–516. [CrossRef]
18. Ertugrul, T.Y.; Celika, S.; Mat, M.D. Optimum processing parameters to improve sealing performance in solid oxide fuel cells. *Ceram. Int.* **2015**, *41*, 9834–9842. [CrossRef]
19. Shi, R.; Liu, J.; Wang, H.; Wu, F.; Miao, H. Intermediate temperature fuel cell durability of Eu-doped $SrCeO_3$-$SrZrO_3$ solid solution/NaCl-KCl composite electrolyte. *Ceram. Int.* **2017**, *43*, 16931–16935. [CrossRef]
20. Sun, L.; Wang, H.; Sheng, L.; Li, H. Gadolinium doped strontium cerate prepared by citric-nitrate auto-combustion process and intermediate temperature electrical properties of its composite electrolyte. *Int. J. Electrochem. Sci.* **2017**, *12*, 9689–9696. [CrossRef]
21. Guan, Q.; Wang, H.; Miao, H.; Sheng, L.; Li, H. Synthesis and conductivity of strontium cerate doped by erbium oxide and its composite electrolyte for intermediate temperature fuel cell. *Ceram. Int.* **2017**, *43*, 9317–9321. [CrossRef]
22. Shi, R.; Liu, J.; Wang, H.; Wu, F.; Miao, H.; Cui, Y. Low temperature synthesis of $SrCe_{0.9}Eu_{0.1}O_{3-\alpha}$ by sol-gel method and $SrCe_{0.9}Eu_{0.1}O_{3-\alpha}$-NaCl-KCl composite electrolyte for intermediate temperature fuel cells. *Int. J. Electrochem. Sci.* **2017**, *12*, 11594–11601. [CrossRef]
23. Zhang, W.; Yuan, M.; Wang, H.; Liu, J. High-performance intermediate temperature fuel cells of new $SrCe_{0.9}Yb_{0.1}O_{3-\alpha}$-inorganic salt composite electrolytes. *J. Alloys Compd.* **2016**, *677*, 38–41. [CrossRef]

24. Matsuda, A.; Oh, S.; Nguyen, V.H.; Daiko, Y.; Kawamura, G.; Muto, H. Anhydrous proton conductivity of $KHSO_4$-$H_3PW_{12}O_{40}$ composites and the correlation with hydrogen bonding distance under ambient pressure. *Electrochim. Acta* **2011**, *56*, 9364–9369. [CrossRef]
25. Soo, M.T.; Prastomo, N.; Matsuda, A.; Kawamura, G.; Muto, H.; Noor, A.F.M.; Lockman, Z.; Cheong, K.Y. Elaboration and characterization of sol-gel derived ZrO_2 thin films treated with hot water. *Appl. Surf. Sci.* **2012**, *258*, 5250–5258. [CrossRef]
26. Miranda, M.I.G.; Bica, C.I.D.; Nachtigall, S.M.B.; Rehman, N.; Rosa, S.M.L. Kinetical thermal degradation study of maize straw and soybean hull celluloses by simultaneous DSC–TGA and MDSC techniques. *Thermochim. Acta* **2013**, *565*, 65–71. [CrossRef]
27. Huang, S.; Sheng, J.J. An innovative method to build a comprehensive kinetic model for air injection using TGA/DSC experiments. *Fuel* **2017**, *210*, 98–106. [CrossRef]
28. Mori, M.; Hiei, Y.; Itoh, H.; Tompsett, G.A.; Sammes, N.M. Evaluation of Ni and Ti-doped Y_2O_3 stabilized ZrO_2 cermet as an anode in high-temperature solid oxide fuel cells. *Solid State Ion.* **2003**, *160*, 1–14. [CrossRef]
29. Yoon, S.; Noh, T.; Kim, W.; Choi, J.; Lee, H. Structural parameters and oxygen ion conductivity of Y_2O_3-ZrO_2 and MgO-ZrO_2 at high temperature. *Ceram. Int.* **2013**, *39*, 9247–9251. [CrossRef]
30. Meng, X.; Gong, X.; Yang, N.; Tan, X.; Yin, Y.; Ma, Z. Fabrication of Y_2O_3-stabilized-ZrO_2 (YSZ)/$La_{0.8}Sr_{0.2}MnO_{3-\delta}$-YSZ dual-layer hollow fibers for the cathode-supported micro-tubular solid oxide fuel cells by a co-spinning/co-sintering technique. *J. Power Sources* **2013**, *237*, 277–284. [CrossRef]
31. Roehrens, D.; Packbier, U.; Fang, Q.; Blum, L.; Sebold, D.; Bram, M.; Menzler, N. Operation of thin-film electrolyte metal-supported solid oxide fuel cells in lightweight and stationary stacks: Material and microstructural aspects. *Materials* **2016**, *9*, 762. [CrossRef] [PubMed]
32. Kusnezoff, M.; Trofimenko, N.; Müller, M.; Michaelis, A. Influence of electrode design and contacting layers on performance of electrolyte supported SOFC/SOEC single cells. *Materials* **2016**, *9*, 906. [CrossRef] [PubMed]